35-4

# AN EXPLORATORY STUDY OF A RIJKE-TYPE, PULSE COMBUSTOR OPERATING WITH GASEOUS AND LIQUID FUELS

**R.K.Dubey, M.Q.McQuay**
Mechanical Engineering Department
Brigham Young University
242 Clyde Building, Provo, UT 84602, USA
mq01@bones.et.byu.edu

**P.T.Lacava, M.A.Ferreira, J.A.Carvalho Jr.**
Laboratorio Associado de Combustao e Propulsao
Instituto Nacional de Pesquisas Espaciais
Rod. Pres. Dutra, Km 40, Cachoeira Paulista, SP, CEP 12630-000, Brazil

presented at

A WORKSHOP IN
PULSATING COMBUSTION AND ITS APPLICATIONS
Mornington, VIC, Australia
10th - 13th April 1995

## ABSTRACT

A study was performed to determine the effect of atomization parameters on the performance of a Rijke-type combustor. This reactor has a length of 3.0 m, is 0.197 m in diameter, has water-cooled walls and an operating range of 50-200 kW. The burner used has horizontally spread arms with several holes for gaseous fuels and a centrally located air-atomizing nozzle for liquid fuels. Average temperatures and acoustic pressure amplitudes are measured using thermocouples and pressure transducers, respectively. Sound pressure level was found to be dependent on oxidant/fuel ratios, mass flow rates and flame position. A maximum sound pressure level of 165 dB was reached at 185 kW at stoichiometric conditions using propane. Sound pressure levels of 170 dB were measured at stoichiometric combustion operating at 200 kW for liquid ethanol. The Sauter-mean diameter for best combustion and maximum sound pressure level was found to be around 45 μm.


## 1.0 INTRODUCTION

The presence of acoustic oscillations in a combustion chamber may be welcome, such as the case of a pulse combustor used in residential heating, or of drastic consequences, such as the case of combustion instabilities in rocket motors. Several aspects of pulse combustion make it attractive over steady-state combustion such as enhanced combustion efficiencies, high heat transfer rates, and reduced pollutant formation. The objective of the exploratory research reported herein is to characterize a new Rijke burner built at Brigham Young University (BYU) as part of a collaboration with the National Institute of Space Research in Brazil (INPE). Measurements of sound pressure amplitude are presented as a function of fuel type, equivalence ratio, power output, and flame position. The effect of droplet Sauter-mean diameter is also investigated qualitatively. The overall objective of this international collaboration is to better understand the influence of atomization parameters on combustion instabilities in pulse combustors. Local, spatially resolved measurements of droplet size, velocity, and number density are planned for the near future using non intrusive, laser-based diagnostics.

Rijke-type combustors have been used extensively to study several aspects of oscillating combustion. The pulse combustor used here has been studied in some detail by Zinn (1982) and coworkers, who used coal as fuel for achieving controlled pulse combustion. Further study on the burning of unpulverized coal and agricultural residues has been done by Carvalho (1987, 1992). Furthermore, Rijke burners have been used in two-phase combustion research to characterize the effect of burning aluminum particles on the growth rate of pressure fluctuations. Recently, Beckstead and coworkers, (1993) have published a literature review on this broad subject. Also, characterized by oscillating droplet combustion, liquid fuel combustion in pulsating environment has been the subject of recent research. See, for example, the recent publications of Blaszcyk (1991), and Saito et al. (1993), dealing with the burning of single droplets in an oscillating flow field. Atomization parameters, such as droplet Sauter-mean diameter, droplet size spectrum and number density, are believed to drive instability; however, little is known about the effect of such spray parameters on the performance of Rijke-type, pulse combustors. The complex nature of the combustion phenomenon in these devices, involving time-dependent heat and pressure fluctuations, mass transport, chemical kinetics and the interdependency of these phenomena, further complicates the problem. The study discussed here is the first to focus on the effect of atomization parameters on the performance of these types of burners.

A few applications of laser diagnostics to pulse combustors are found in the literature. Loizeau and Gervais (1994) have made measurements of acoustic and mean velocity in a Rijke Tube using Laser Doppler Velocimetry for an evaluation of the unsteady nature of heat release and comparison with mathematical model predictions. Lindholm (1993) has made flow field measurements in a pulse combustor with a square cross section of the combustion chamber, using LDV for comparison with computer simulations. Moller (1993) has made measurement of the velocity flow field in a flat pulse combustor for comparison with a CFD code simulation. Lindholm et al (1991) have made measurements in a pulse combustor using LDV for velocities and CARS for temperatures. However, no work can be found focusing on the effect of atomization parameters on the performance of Rijke burners.

## 2.0 EXPERIMENTAL FACILITY

The Rijke-type pulse combustor used for the present exploratory study was first characterized using gaseous propane fuel. Sound pressure amplitude and frequency variations were measured at different reactor power settings ranging from 50 to 200 kW. A liquid ethanol spray was then successfully used to obtain pulsating combustion in the reactor. There were some problems of flame blowout and instability during combustion with liquid ethanol, which was found to be dependent on the nozzle atomizing conditions. This effect is believed to be dependent on the transport mechanism and mixing involved in droplet combustion, discrete in nature and sensitive to fuel type and injector design.

Figure 1 displays a schematic of the Rijke burner used. The reactor was built with modular sections, allowing the reactor height to be systematically varied from 1.2 to 3.0 m. In the current configuration, the height of the reactor is 3.0 m and the diameter is 0.197 m. The outer wall of the combustor is water cooled and can be used to control the amount of heat transferred to the walls. The tube is open at the top and the entire combustor is placed on a cubic decoupling chamber (1 m on the side). Pressure monitoring ports exist at L/4 and 3L/4, where L is the length of the tube, for measuring the frequency and level of the fluctuating pressure signal. The combustor has two optical quartz windows, oriented at an angle of 120 degrees, for photographing the flame and providing access for the Phase Doppler Particle Analyzer (PDPA) instrument to be later used. This instrument is capable of measuring droplet size (in the range of 0.5 to 500 $\mu$m), velocity (two components), and number density (up to $10^6$ particles/$cm^3$) in reacting and nonreacting flows. Information provided by this laser system is size resolved. Nozzle characterization was done using the PDPA instrument outside the reactor for similar conditions of air and liquid flow using water. Local measurements inside the pulse combustor are planned for the near future.

The temperature of the exhaust is monitored using S-type thermocouples. The primary air for combustion is supplied from a blower, rated at 9 $m^3$/min capacity, through the bottom of the decoupling chamber. The air expands in the chamber and attains an uniform velocity profile while entering the main tube of the combustor. It passes through a wire screen, located just below the flame holder, before mixing with the fuel for combustion. The wire screen introduces local turbulence, helping the mixing process for efficient combustion and providing the initial instability for the pulse combustion to be established. The flow rate of the air is measured using an orifice plate. The pressure drop across the orifice and the upstream pressure are measured using Omega pressure transducers model PX142 and PX170, respectively, and the upstream air temperature is measured using a K-type thermocouple. An empirical correlation found in Miller's handbook (1983) is then used to determine the air flow rate.

Figure 2 displays a schematic of the burner and positioning device. As seen in the figure, the burner is comprised of two parts. The first part consists of 10 spatially distributed, horizontal arms with small holes for gaseous fuel. The second part is a Delavan AIRO solid-cone, air atomizing nozzle (model 30615) located at the center of the flame holder for liquid fuel. Gaseous propane from a pressurized tank is used for combustion. It's volume flow rate is measured with an Omega (model FL3840) flowmeter. Upstream pressure and temperature are measured for calculating the mass flow rate from the volume flow rate. Liquid ethanol flow rate through the nozzle is measured in a similar fashion. A separately monitored secondary source of high pressure air is used for atomizing the liquid fuel in the nozzle. The nozzle is capable of producing liquid droplets in the range of 10 to 150 $\mu$m. The entire burner assembly is located on a positioning device which can be controlled from outside to vary the location of the flame holder from L/8 to L/2 in the Rijke combustor. Flame blowout and extinction led to a simple modification in the flame holder design. A circular plate was placed just below the nozzle to create a recirculation zone thus stabilizing the flame and preventing blowout. Also, a bluff body, located at a height of 5 cm from the nozzle was installed, acting as an instantaneous source of heat for re-igniting the fuel and helping to maintain stability during combustion. The problem with this modification is that it lead to a droplet size distribution during combustion different than the one obtained through the characterization of the nozzle outside of the reactor under the same operating conditions using the PDPA system. This problem will be circumvented in later studies by performing in-situ nozzle characterization and by using a swirling nozzle for flame stabilization. However, it is believed that the results presented here on the effect of droplet Sauter-mean diameter will preserve their qualitative character.

Pressure fluctuations are monitored using two Kistler pressure transducers (model 7261) with a sensitivity of 2200 pC/bar, positioned at L/2 and 3L/4. The signal coming from the transducer is then converted and displayed on a Tektronix oscilloscope model TD420 using a charge amplifier. Preferred frequencies in the pressure fluctuation signals are directly read from the oscilloscope in Hz. Reactor power is calculated from the calorific value and the mass flow rate of the fuel in a spreadsheet used to evaluate the data gathered during experimentation. This simple program analyzes all inputs and displays the equivalence ratio, power in kW, sound pressure level in dB, frequency in Hz, and the flame position inside the reactor.

## 3.0 RESULTS AND DISCUSSION

This section presents and discusses the results of the exploratory study on the effects of atomization parameters on the Rijke-type pulse combustor previously described. Three basic studies have been performed. The first one is a characterization of the reactor using gaseous propane. The second study repeats this characterization using a liquid ethanol flame and the third looks at the qualitative effects of atomization on combustion-driven oscillation in the Rijke combustor. The flame structure observed during the study discussed here was highly turbulent. Its length has been found to decrease with oscillations. The results presented herein are introduced in the order mentioned in this paragraph.

### 3.1 Gaseous Propane Data

Pressure fluctuations and flame structure of the gaseous propane flame are very stable compared to those of the ethanol flame. This is due to the enhanced mixing of the fuel and the oxidant caused by the intricate burner design. The flame is short and mostly yellow. Figure 3 shows the effect of equivalence ratio on the Sound Pressure Level (SPL) inside the combustor for four different reactor power settings with the burner maintained at 0.53 m for all the tests. Here, the normalized air/fuel ratio is defined as the ratio of actual to stoichiometric air/fuel ratios -- thus a value greater than one indicates an overall lean flame. As observed in Fig. 3, the SPL peak increased in magnitude and shifts towards stoichiometric conditions as the reactor power increased. The normalized air/fuel ratio range shortened as power increased and in general most oscillations were observed for lean conditions. The increase in SPL peak magnitude with reactor power can be attributed to the fact that, with the increase in reactor power, more energy is available to drive the pressure oscillations. The reason for the shift towards stoichiometry is based on the fact that the oscillations are strongest when the heat release and the pressure wave are in phase. This phase is dependent on the total flow rate and the mass burning rate, which in this case is dependent on the power of the reactor, McIntosh (1993). At lower power, the fuel flow rate is reduced, so to reach the same level of total flow conditions as with the higher power, more air flow is required.

Another thing to notice in Fig. 3 is the narrowing of the data band as the power of the reactor increases. This is dependent on three factors, namely the fuel flow, turbulence and the total flow rate. Now the leftmost data point at each power setting is dependent on the fact that as the excess air decreases, the flame becomes long and heat distribution is no longer in the lower half of the reactor causing the oscillations to stop, and the rightmost data point is dependent on blow off due too high turbulence and flow rate. Thus one can say that at higher power, due to higher fuel flow rate, the flame becomes longer than L/2 at a faster rate than that at the lower power and also at higher power, due to high turbulence and flow rate, it has tendency to blow off faster than that at lower power. This explains the fact that the data band becomes narrow as the power increases.

To study the effect of flame position inside the Rijke tube on oscillation for the gaseous propane flame, the power of the reactor was set at 80 kW and the propane-air mixture was introduced at stoichiometric conditions. The burner position was varied from 45 cm to 65 cm from the bottom of the tube and the SPL was measured, as shown in Fig. 4. The center measurements showed a maximum SPL of 163 dB at a burner position of 57 cm from the bottom, which corresponds to a flame center location near 75 cm (L/4). Frequency was found to increase slightly with power and a variation of 4 Hz was observed over a power range of 50 to 200 kW as shown in Fig. 5. It should be noted that this slight increase in frequency may also have been caused by a change in exhaust gas temperature (changing the speed of sound in the hot section of the reactor) with time rather than a change in flame position.

### 3.2 Liquid Ethanol Data

Figure 6 shows the effect of equivalence ratio on SPL using ethanol fuel for two different power settings (75 and 115 kW). The burner was kept at the same 0.53-m position in these tests. The pattern observed in this graph is similar to that observed in Fig. 3. A data set as complete as the one shown in Fig. 3 was not obtained for the spray flame because of instability and blowout problems, but the trends seem to indicate that the SPL peak increases with power and shifts towards the stoichiometric conditions as the reactor power increased. However, the increase in SPL peak magnitude with reactor power is not as large as the ones observed for the gaseous flames. Note also that, for similar reactor power levels, the SPL peak takes place at leaner conditions for the liquid fuel as compared to the gaseous flame (compare the 77- and 123-kW curves in Fig. 3 to the 75- and 115- kW curves in Fig. 6, respectively).

The effect of flame position on the SPL seems to follow similar trends for the ethanol flame. A maximum SPL of 168 dB was measured at a flame position around L/4 in the tube (Fig. 7). This dependence is expected in accordance to the predictions of Rayleigh's criterion. Notice however that a more distinct peak in the curve is observed in the liquid fuel case, indicating a flame more sensitive to position than the gaseous flame.

Figure 8 shows the effect of equivalence ratio on the frequency of oscillations. A dome shaped variation is observed at a power setting of 115 kW, with a peak frequency of 77 Hz at around $\phi$ = 1.45. This can be attributed to the fact that with an increase in equivalence ratio, heat input decreases which results in a decrease of frequency, but as the air/fuel mixture becomes richer, the flame has a tendency to elongate causing higher temperatures in the hot region of the combustor, decreasing the frequency.

### 3.3 Effect of Atomization Parameter

The nozzle used for spray combustion in this study was characterized outside the reactor with water for similar flow conditions. In-situ measurements have been planned and will be soon conducted. Furthermore, due to flame stability problems as previously discussed, the use of an impingement plate was inevitable, causing the spray characterization to change in the reactor compared to the cold-flow cases characterized outside the reactor using water. However, it is believed that the same qualitative behavior of the spray characterization is obtained as the liquid and air flow rates in the nozzle are changed. Figure 9 shows the effect of Sauter-mean diameter (D32) on the sound pressure level. The SPL is observed to increase with increase in droplet size and then drops off after reaching a peak level of 168.7 dB at 45 microns. This suggests that the pressure oscillation is strongly dependent on the droplet diameter and velocity profiles.

## 4.0 CONCLUDING REMARKS

An experimental study to characterize a new Rijke combustor and to determine the effect of atomization parameters on spray combustion was performed. A comparison between gaseous combustion flame and liquid droplet flame has been made, and it has been shown that there are more instabilities present for a liquid droplet flame. It has also been found that the sound pressure level is dependent on the intensity of heat release inside the combustor. It has been found that the acoustic wave present inside the combustor is strongly dependent on the Sauter-mean diameter of the liquid fuel droplets.

## 5.0 ACKNOWLEDGMENT

This work was sponsored by the Advanced Combustion Engineering Research Center (ACERC) located at Brigham Young University, the National Science Foundation of the United States and the Combustion and Propulsion Associate Laboratory located at the National Space Research Institute, Brazil.

## 6.0 REFERENCES

Arcoumanis, C.,'In-Cylinder flows and implications for combustion in spark ignition engines', L25, Advanced study institute on Unsteady Combustion, 1993

Blaszczyk, J. "Acoustically Disturbed Fuel Droplet Combustion." Fuel, 70:1023-1025 (1991).

Carvalho Jr, J. A., Miller, N., Daniel, B. R. et al. Fuel, 66, 4, 1987

Carvalho Jr. J. A., Miller, N., Daniel, B. R. et al. Fuel, 66, 4, 1987

Kumagai, S., and Isoda, H. "Combustion of Fuel Droplets in a Vibrating Air Field," 5th International Symposium on Combustion, pp 129-132, (1955)

Lindholm,A.,Naslund,A.,Klingmann,J., and Nilsson,U., ' Measuremnts on Experimental Pulse Combustors at Lund Institute of Technology',Proceedings of The International Symposium on Pulsating Combustion, Vol-1, Aug 5-8, 1991

Lindholm,A., ' Experimental Investigations on a Flat Pulse Combustor',NATO Advanced Institute on Unsteady Combustion, Sep. 6-17, 1993

Loizeau,T. and Gervais,Y., 'Measurement of acoustic velocity using Laser Anemometry in a Rijke tube', Journal de Physique, V4, N5, P2, 973-976 (1994)

McIntosh,A.C.,'The Linearised response of the Mass Burning Rate of a Premixed Flame to Rapid Pressure Changes',Combustion Science and Technology,Vol. 91, pp. 329-346,1993

Moller,S.I., 'Numerical Simulation of a Flat Pulse Combustor',NATO Advanced Institute on Unsteady Combustion, Sep. 6-17, 1993

Raun, RL.,Beckstead, MW.,Finlinson, JC., and Brooks, KP., 'Review of Rijke tubes, Rijke burners and related devices',Progress in Energy and Combustion Science v 19 n 4 1993, p 313-364.

Raun, RL., and Beckstead, MW.,'Numerical model for temperature gradient and particle effects on Rijke burner oscillations', Combustion and Flame v 94 n 1-2 Jul 1993, p 1-24.

Saito, M., Sato, M., and Suzuki, I. Evaporation and Combustion of Single Fuel Droplet in Acoustic Fields,"Fuel, 73:349-353 (1994).

Torres,E.A., Victorio, J.R.S., Ferreira, M.A. and Carvalho Jr. J.A., 'Pulsating combustion of palm oil fruit bark', Fuel, 71, 1992

Zinn, B. T., Miller, N. and Carvalho Jr. J. A. et al.'Proc. of the Nineteenth Symposium (International) on Combustion', The Combustion Institute, p. 1197, 1982

# LIST OF FIGURES

**Figure** **Description of the figure**

1. Schematic diagram of the Rijke-type pulse combustor facility located at Brigham Young University.

2. Schematic diagram of the burner.

3. Sound pressure level as a function of overall normalized air/fuel ratio for different reactor power setting using gaseous propane fuel.

4. Profile of sound pressure level as a function of burner position in the Rijke tube for gaseous propane fuel.

5. Frequency variation as a function of reactor power for gaseous propane fuel.

6. Sound pressure level as a function of overall normalized air/fuel ratio at two different power stetting using liquid ethanol fuel.

7. Profile of sound pressure level as a function of burner position in the Rijke tube for liquid ethanol fuel.

8. Frequency variation as a function of overall normalized air/fuel ratio using liquid ethanol fuel.

9. Effect of sauter mean diameter on the sound pressure level in the Rijke tube combustor for liquid ethanol fuel

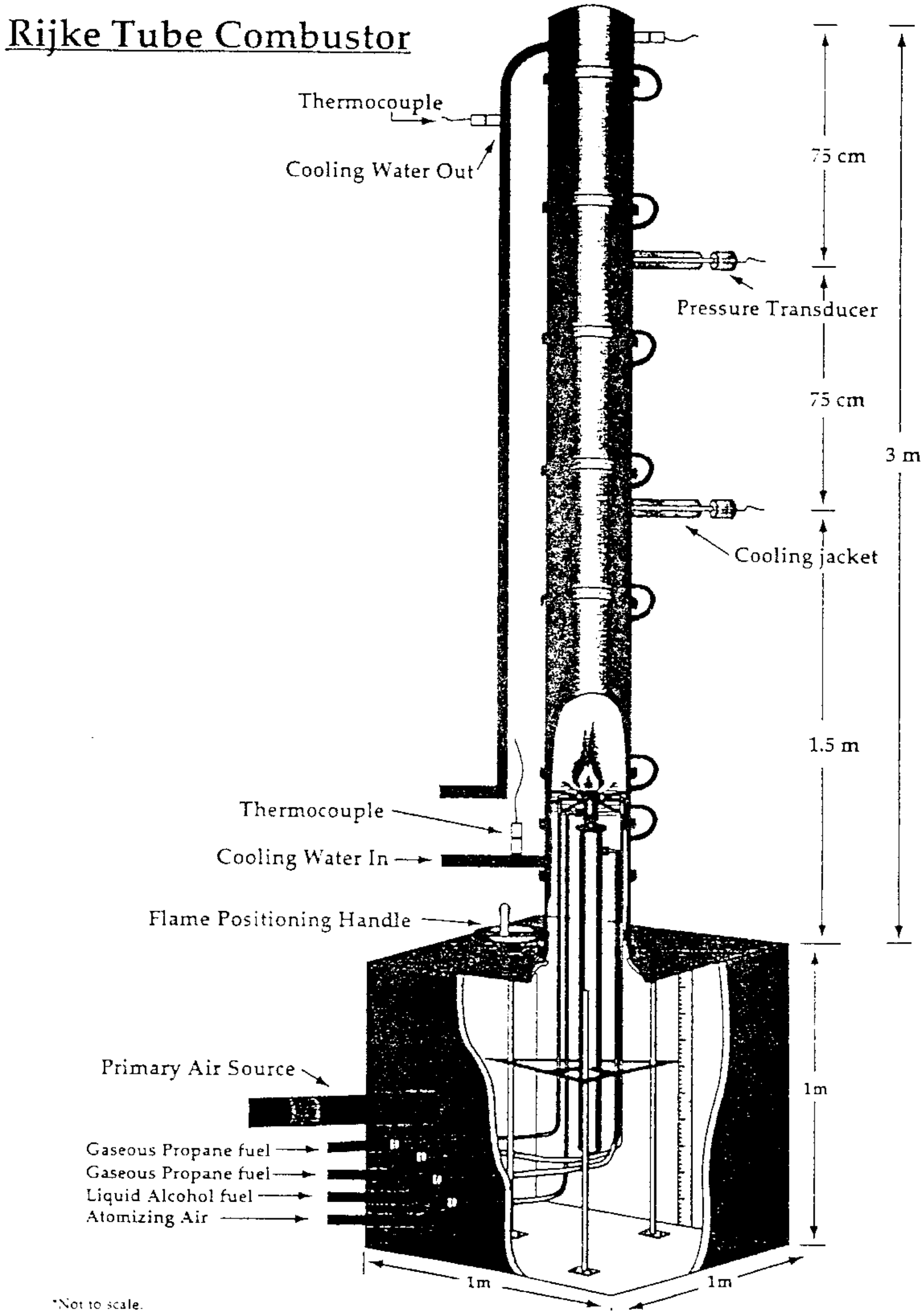
Rijke Tube Combustor
Thermocouple
Cooling Water Out
75 cm
Pressure Transducer
75 cm
3 m
Cooling jacket
1.5 m
Thermocouple
Cooling Water In
Flame Positioning Handle
Primary Air Source
1m
Gaseous Propane fuel
Gaseous Propane fuel
Liquid Alcohol fuel
Atomizing Air
1m
1m
*Not to scale.

Figure 1

# Flame Holder

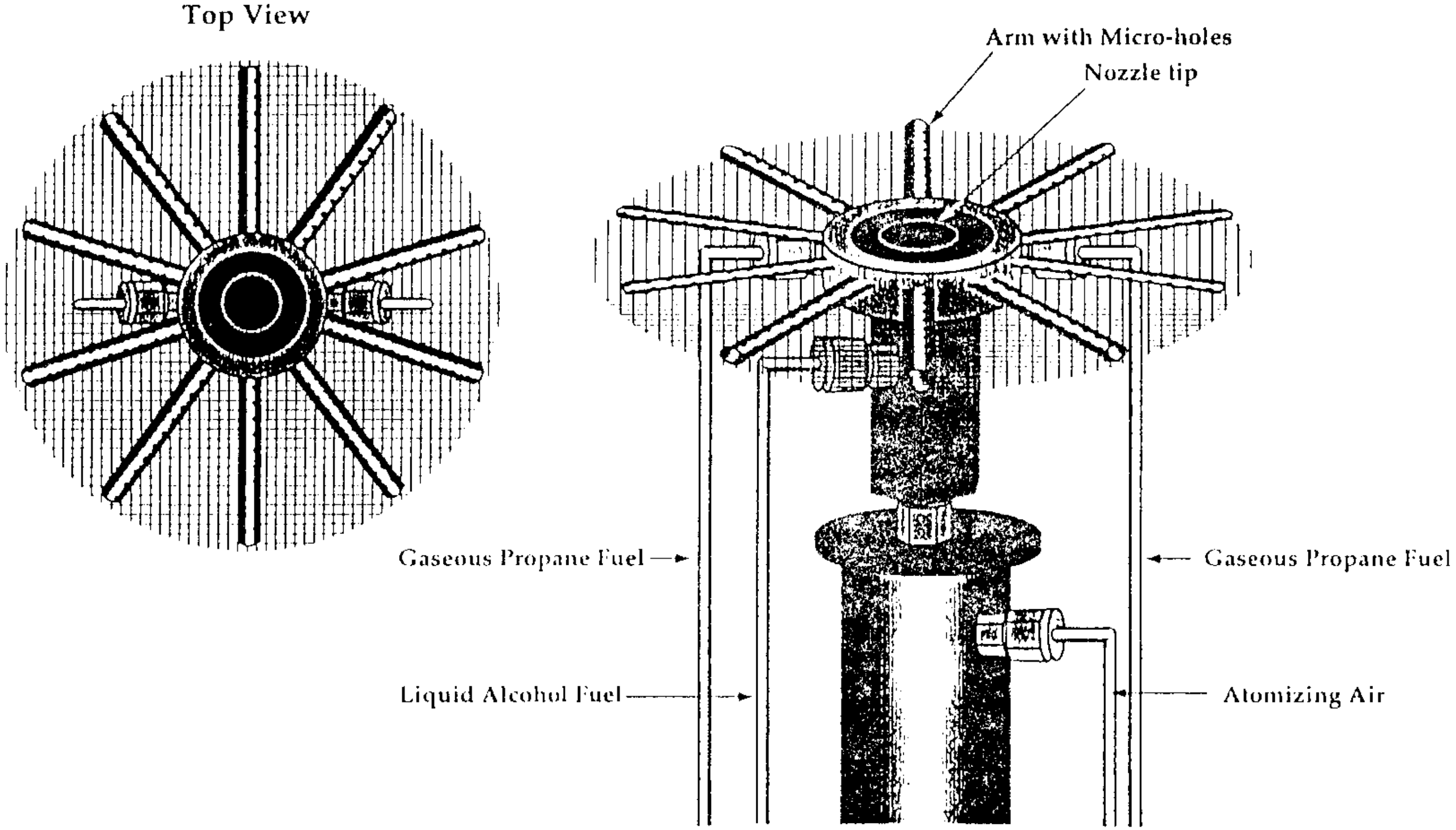


Figure 2

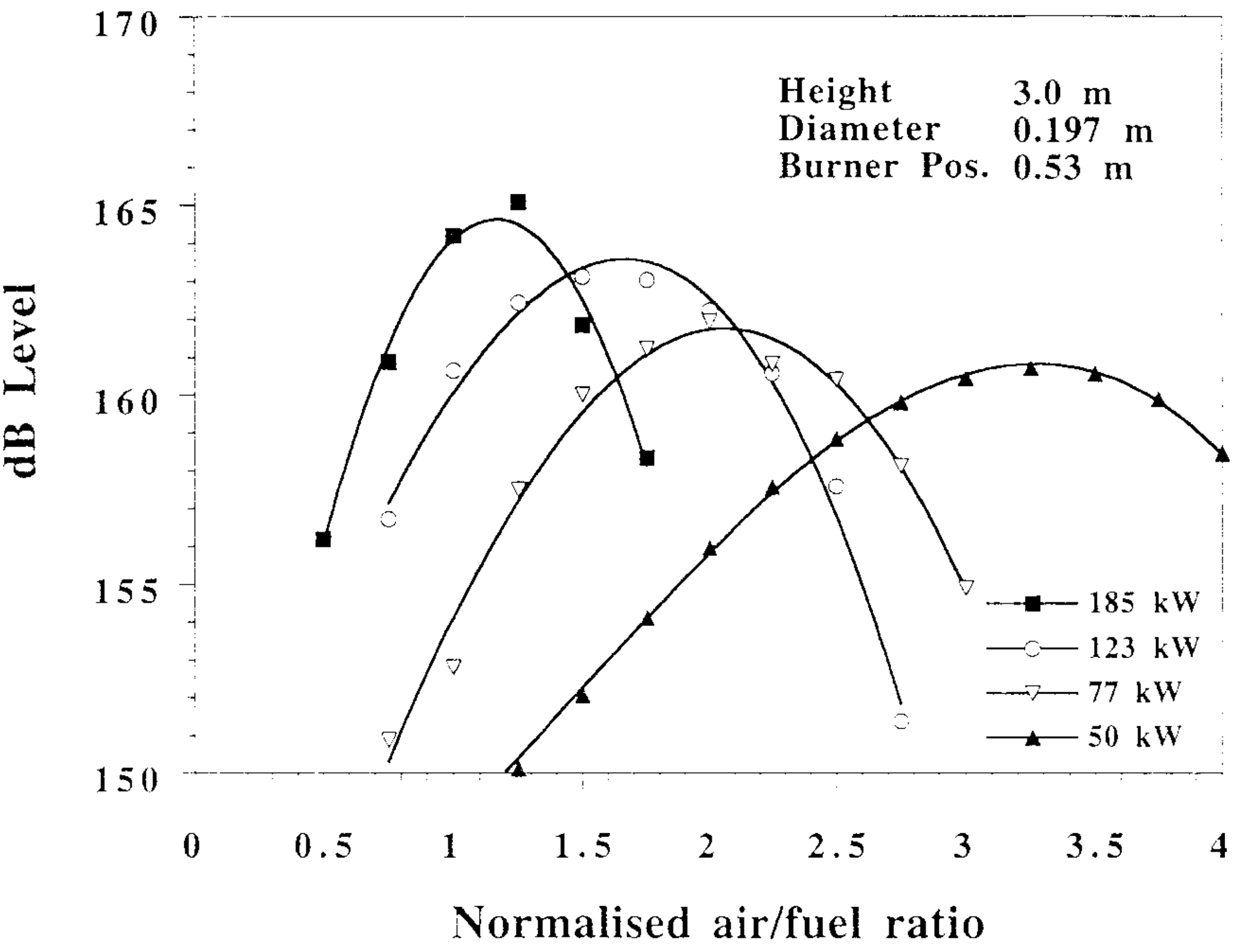

dB Level
170
165
160
155
150
Height 3.0 m
Diameter 0.197 m
Burner Pos. 0.53 m
185 kW
123 kW
77 kW
50 kW
0
0.5
1
1.5
2
2.5
3
3.5
4
Normalised air/fuel ratio


Figure 3

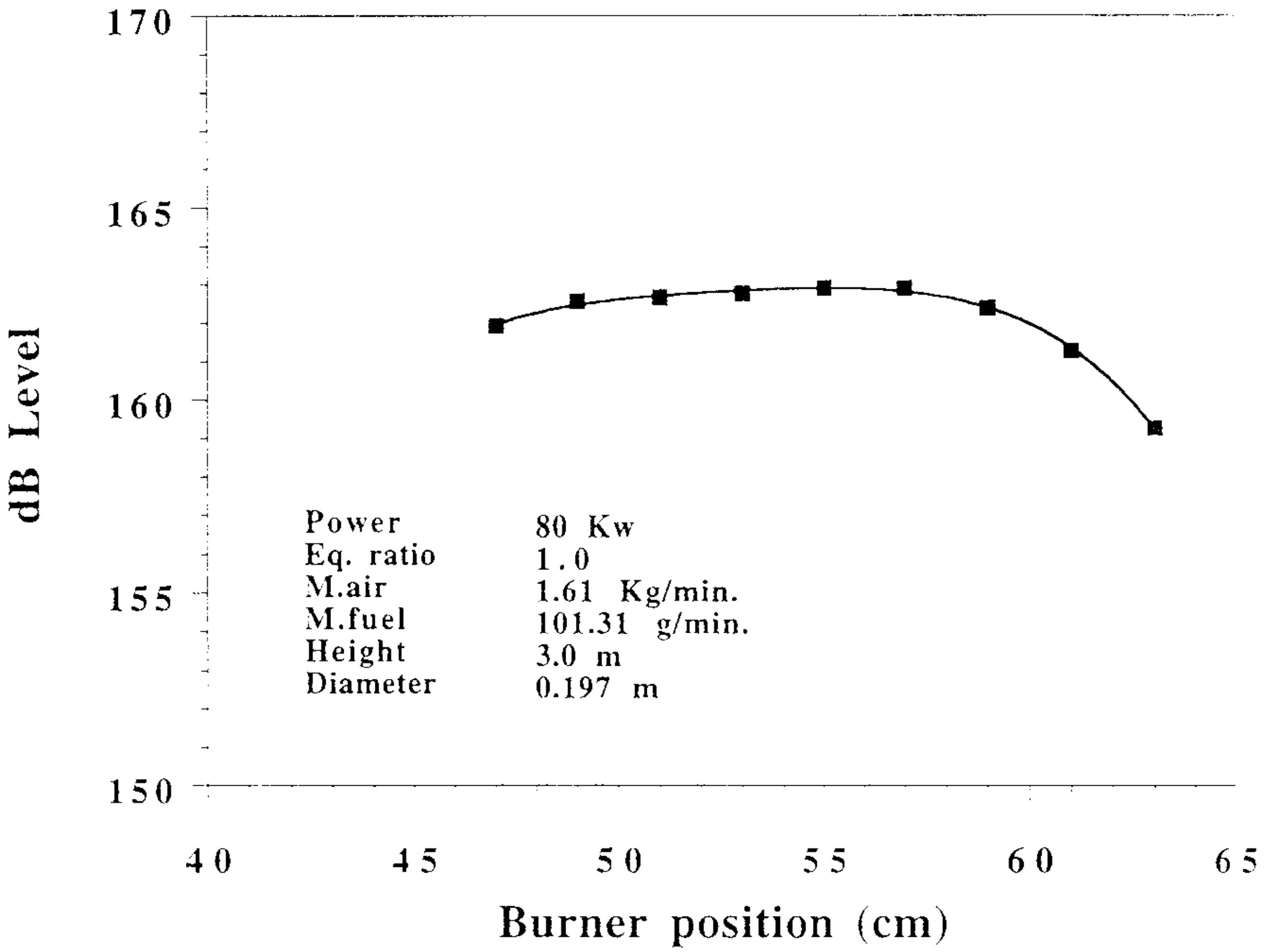
170
165
160
155
150
dB Level
Power
80 Kw
Eq. ratio
1.0
M.air
1.61 Kg/min.
M.fuel
101.31 g/min.
Height
3.0 m
Diameter
0.197 m
40
45
50
55
60
65
Burner position (cm)

Figure 4

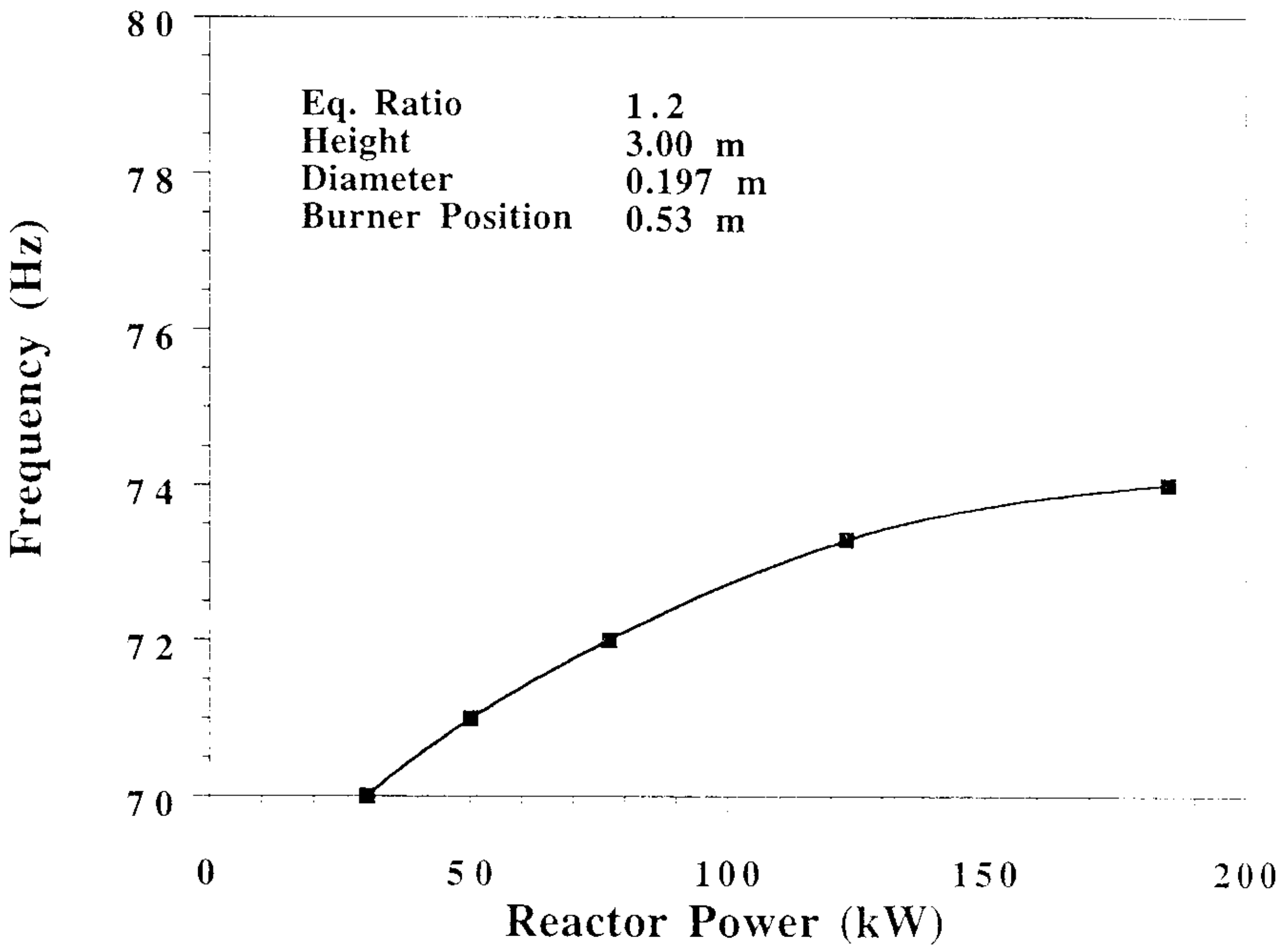
Eq. Ratio 1.2
Height 3.00 m
Diameter 0.197 m
Burner Position 0.53 m
Frequency (Hz)
80
78
76
74
72
70
0
50
100
150
200
Reactor Power (kW)

Figure 5

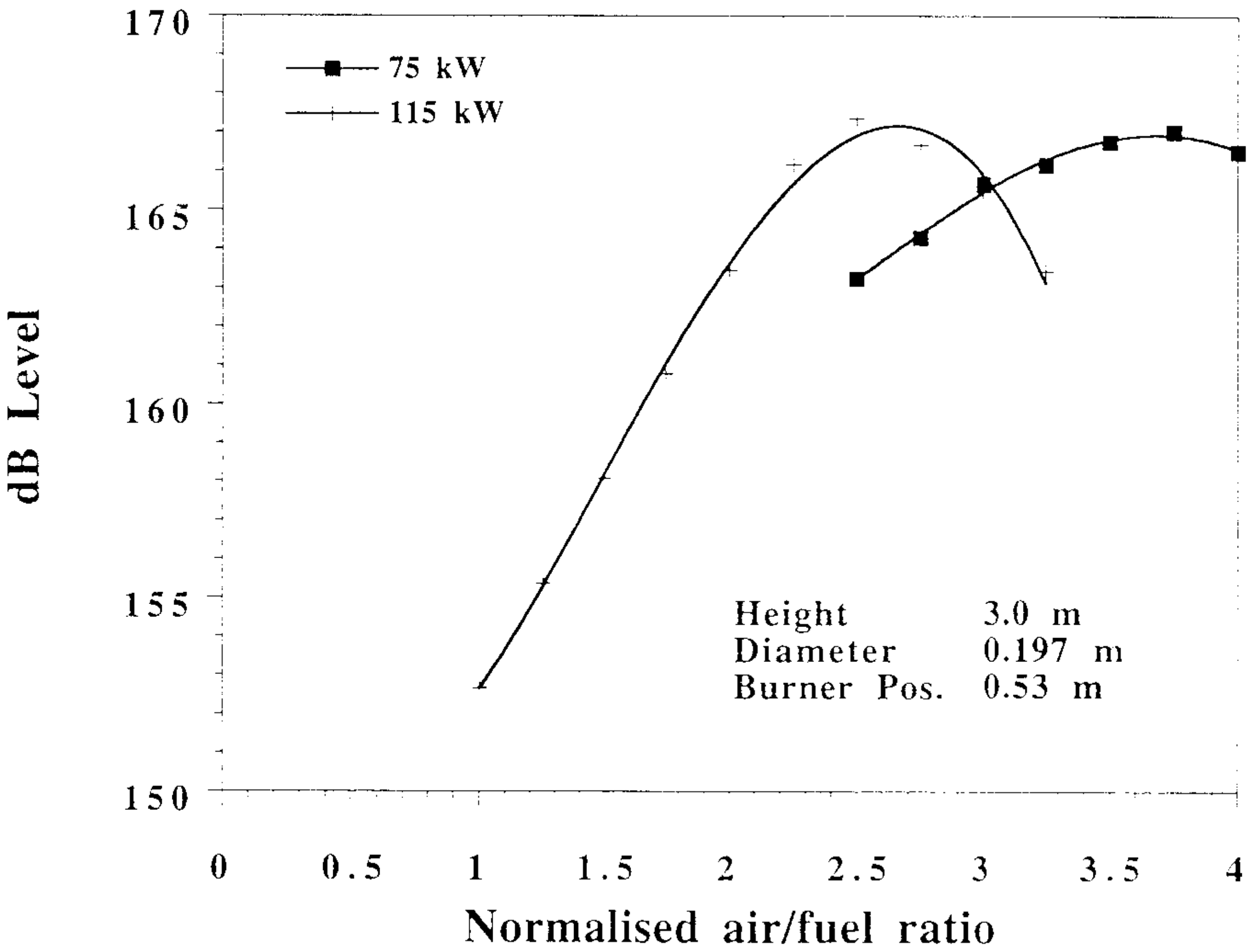

75 kW
115 kW
170
165
160
155
150
dB Level
Height 3.0 m
Diameter 0.197 m
Burner Pos. 0.53 m
0
0.5
1
1.5
2
2.5
3
3.5
4
Normalised air/fuel ratio


Figure 6

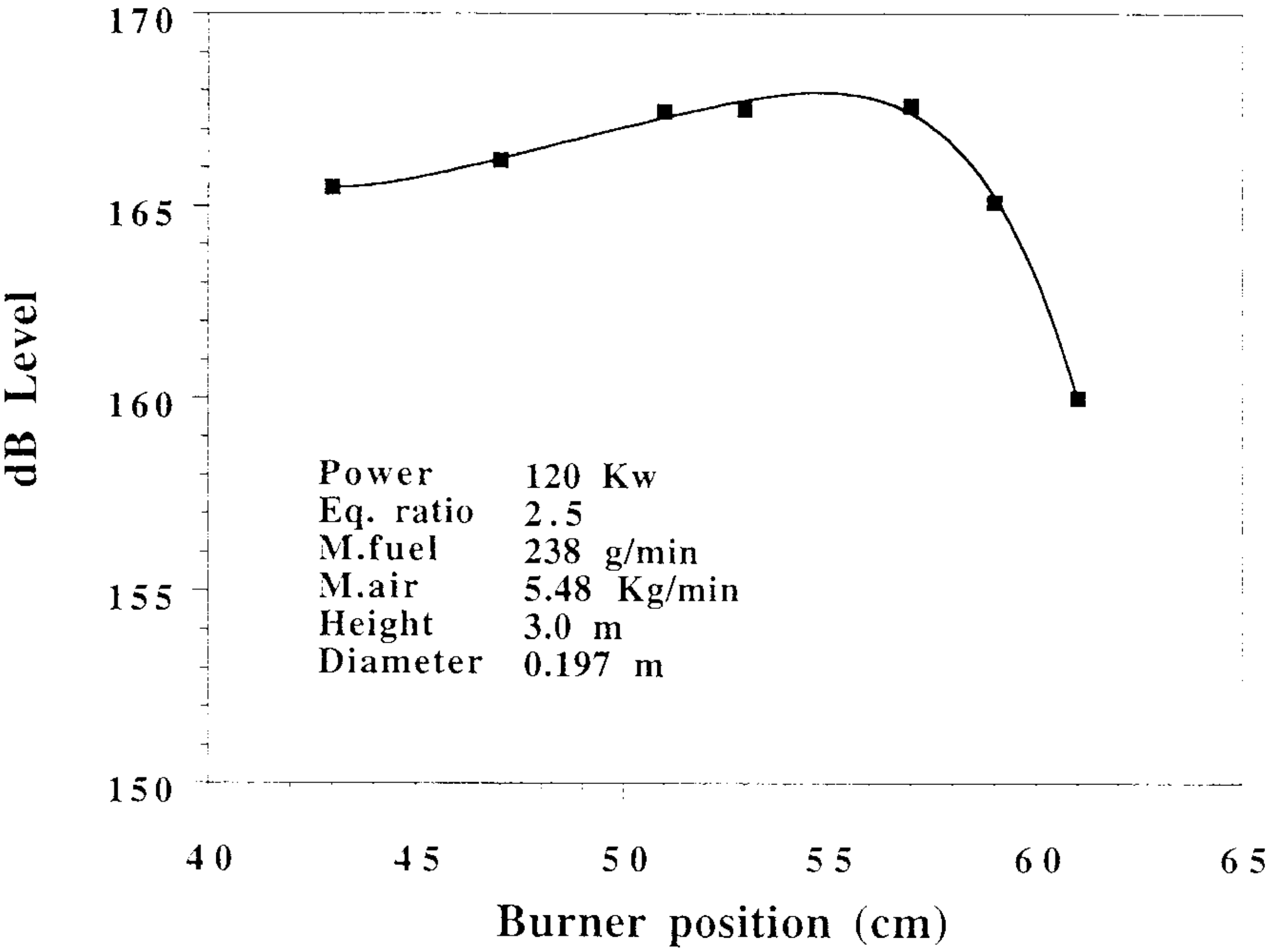

170
165
160
155
150
dB Level
40
45
50
55
60
65
Burner position (cm)
Power 120 Kw
Eq. ratio 2.5
M.fuel 238 g/min
M.air 5.48 Kg/min
Height 3.0 m
Diameter 0.197 m


Figure 7

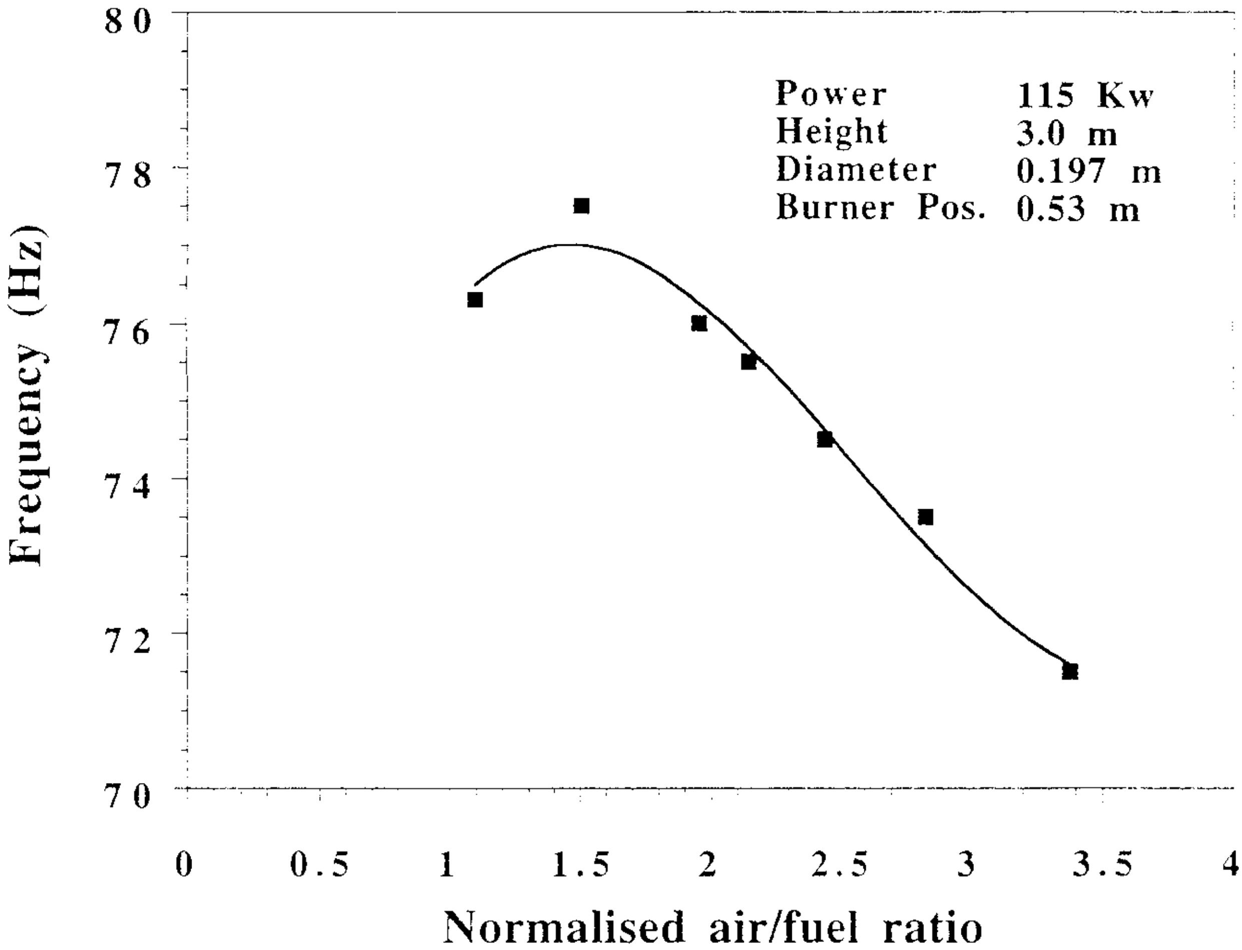
Power 115 Kw
Height 3.0 m
Diameter 0.197 m
Burner Pos. 0.53 m
Frequency (Hz)
80
78
76
74
72
70
0
0.5
1
1.5
2
2.5
3
3.5
4
Normalised air/fuel ratio

Figure 8

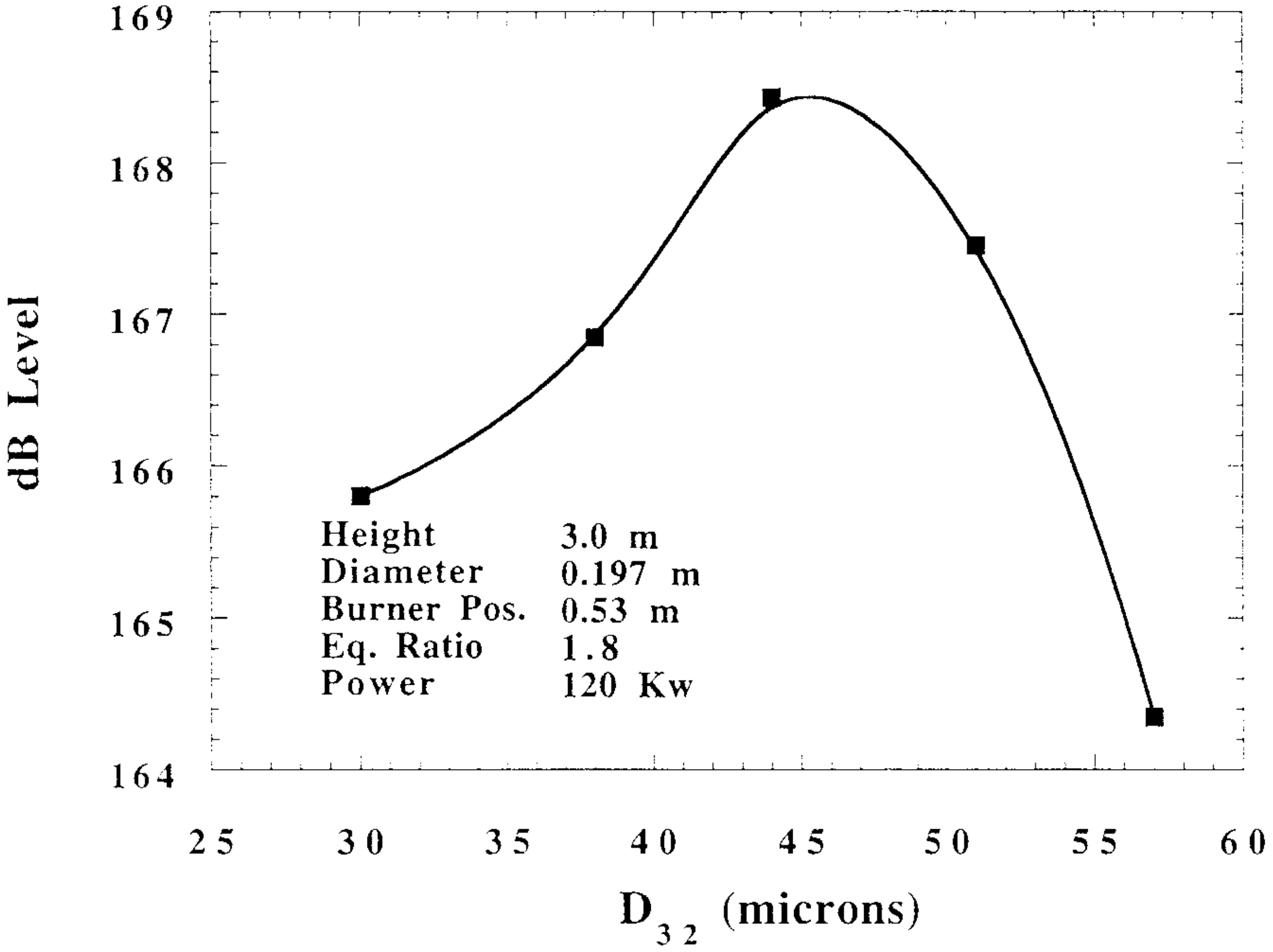
169
168
167
166
165
164
dB Level
Height 3.0 m
Diameter 0.197 m
Burner Pos. 0.53 m
Eq. Ratio 1.8
Power 120 Kw
25
30
35
40
45
50
55
60
D32 (microns)

Figure 9